Journal of Applied Polymer Science

Lignocellulosic Jute Fiber as a Bioadsorbent for the Removal of Azo Dye from Its Aqueous Solution: Batch and Column Studies

Aparna Roy, Sumit Chakraborty, Sarada Prasad Kundu, Basudam Adhikari, Subhasish Basu Majumder*

Materials Science Centre, Indian Institute of Technology Kharagpur, West Bengal 721302, India

*Correspondence to: S. B. Majumder (E-mail: subhasish@matsc.iitkgp.ernet.in)

ABSTRACT: The feasibility of the use of jute fiber for the adsorption of azo dye from an aqueous solution was evaluated with batch and fixed-bed column studies. The batch studies illustrated that dye uptake was highly dependent on different process variables, namely, the pH, initial dye concentration of the solution, adsorbent dosage, contact time, ionic strength, and temperature. The exothermic and spontaneous nature of adsorption was revealed from thermodynamic study. The equilibrium adsorption data were highly consistent with the Langmuir isotherm and yielded an R^2 value of 0.999. Kinetic studies divulged that the adsorption followed a pseudo-second-order model with regard to the intraparticle diffusion. In the column studies, the total amount of adsorbed dye and the adsorption capacity decreased with increasing flow rate and increased with increasing bed height and initial dye concentration. Also, the breakthrough time and exhaustion time increased with increasing bed depth but decreased with increasing flow rate and influent dye concentration. The column performances were predicted by the application of the bed-depth service time model and Thomas model to the experimental data. The virgin and dye-adsorbed jute fiber was characterized by Fourier transform infrared spectroscopy and scanning electron microscopy analyses. The investigation suggested that jute fiber could be applied as a promising low-cost adsorbent for dye removal. © 2012 Wiley Periodicals, Inc. J. Appl. Polym. Sci. 000: 000–000, 2012

KEYWORDS: adsorption; biopolymers; dyes/pigments; fibers; renewable resources

Received 1 April 2012; accepted 21 June 2012; published online
DOI: 10.1002/app.38222

INTRODUCTION

Nowadays, one major environmental issue is the increasing worldwide pollution of freshwater systems with hazardous industrial chemical compounds.[1] Among various organic or inorganic pollutants, dyes are also common contaminants that pose a major threat to the environment. A huge volume of toxic wastewater with highly colored synthetic dyes are discharged to the environment from different dyestuff manufacturing and using industries, including the textile, leather, paper, petroleum, printing, cosmetics, paint, pigments, rubber, plastic, pesticide, wood preserving chemicals, food, and pharmaceutical industries.[2] The presence of dyes, even at very low concentrations, imparts color to water systems and restricts their beneficial use.[3] The discharge of colored effluents into aquatic systems increases chemical oxygen demand and dissolved and suspended solids and also impedes light penetration into water. This, in turn, creates interference for the photosynthesis of aquatic plants, hinders the growth of microbes, and eventually results ecological inequity in water bodies. Dye-polluted water is also harmful to human beings and animals because of the carcinogenic, mutagenic, allergic, and toxic nature of dyes and their metabolites.[4] The dyes are highly stable and complex organic molecules and, thus, are difficult to degrade by means of oxidizing agents, light, heat, and microbial attacks. Dye-contaminated wastewater can be treated by various techniques, such as coagulation and flocculation, ozonation, membrane-filtration processes, ion exchange, and chemical precipitation. However, these techniques have several disadvantages, including inefficiency at lower concentrations, the requirement of a high energy and reagents, the generation of toxic sludge or other wastes as byproducts that need careful treatment and disposal, high capital and operational costs, and labor intensiveness.[5] In these circumstances, the removal of toxic dyes from wastewater emerges as a major challenge. Accordingly, adsorption has been proven to be an efficient and reliable alternative dye-removal process to available wastewater treatment techniques because of its simple design and low initial investment cost. Among a large variety of adsorbents, activated carbon is most widely used because of its

Additional Supporting Information may be found in the online version of this article.

excellent adsorption ability. However, its use is restricted, at least in developing countries, because of its high cost. Thus, this constraint has rendered the application of industrial waste, natural material, or agricultural byproducts as adsorbents. These materials are inexpensive, simple, and abundantly available. Such low-cost adsorbents have satisfactory performance on the laboratory scale for dye adsorption from aqueous solution.[6]

Azo dyes, generally, members of the anionic category, are of extreme environmental concern on account of their bright color, ability to irritate the skin, eyes, and gastrointestinal tract, and well-known human carcinogenic and mutagenic nature.[7] In this context, in recent years, several authors have reported various kinds of low-cost agricultural materials as dye adsorbents, for example, straw, phoenix leaf powder, rice husk, chitosan, peanut husk, jackfruit leaf powder, grape stalk waste, and so on.[1–9] However, the main problem associated with those aforementioned bioadsorbents is their nonabundant availability in the global market; this eventually makes them incapable of meeting the huge commercial demand. On other hand, most researchers have investigated dye adsorption with various low-cost adsorbents by a batch process only.[8] Batch experiments basically evaluate the equilibrium adsorption capacity (q_e) of adsorbents for adsorbates present in aqueous phases.[9] However, the data obtained from such batch methods are generally not applicable to the practical operation of full-scale biosorption processes by continuous-flow, fixed-bed columns because, in column operations, the contact time is not sufficient enough for the attainment of equilibrium. The adaptability of column systems to versatile processes, low reagent handling, and accordingly low operational costs make column techniques popular for the removal of hazardous materials from industrial effluents.[9,10] Thus, equilibrium studies using columns need to be performed before the design and optimization of fixed-bed column operations.[8]

Considering all these facts, in this article, we report on the cost-effective removal of anionic azo dye from aqueous solution using low-cost, renewable, and abundantly available jute fiber. Jute, a lignocellulosic bast fiber, is produced from plants in the genus *Corchorus,* species *olitorius.* Jute fiber contains stable matrix of cellulose, hemicellulose, and lignin, which consists of various active functional groups, such as hydroxyl, carbonyl, and ether, that can make the adsorption process feasible. The largest jute-producing countries are India (mainly West Bengal), Bangladesh, China, and Myanmar. It is one of the cheapest natural fibers and is second only to cotton, in terms of usage, global consumption, production, and availability. Currently, a significant effort is being undertaken to explore the possible utilization of this locally produced lignocellulosic fiber for socioeconomic development. Jute stick powder[11] and activated carbon prepared from jute sticks[12] have already been used as adsorbents for the removal of dyes. However, to the best of our knowledge and belief, no work has been reported on dye adsorption by jute fiber. Jute fiber can be incinerated and disposed of after use without expensive regeneration as it is abundantly available and low in cost. In this study, the performance of jute fiber on dye adsorption in batch and continuous fixed-bed column operations was evaluated. A systematic investigation of the effects of the initial pH, adsorbent dose, temperature, and initial dye concentration (C_0) of the solution on dye uptake were explored in the batch study. Furthermore, breakthrough studies were carried out at different bed depths (Z's), volumetric flow rates (F's), and C_0's. The plausible dye–adsorbent interaction during adsorption in a single-component system was studied in this investigation.

EXPERIMENTAL

Materials

Congo Red (CR) and Stock Solution. CR {1-napthalenesulfonic acid 3,3-[4,4-biphenylene bis(azo)]bis(4-aminodisodium) salt} was considered a model anionic azo dye for this study. It was supplied by Loba Chemicals (Guaranteed Reagent (GR) grade, India). A stock solution of CR in deionized water (1000 mg/L) was prepared. The working solutions were prepared by the dilution of the stock solution with deionized water.

Preparation and Characterization of the Adsorbent. Jute fiber was collected from Gloster Jute Mill (Howrah, India). The long fibers were chopped to about 5 mm in length; washed with deionized water, and dried in an oven. The dried fibers were cooled and stored in an airtight container.

A Fourier transform infrared (FTIR) spectroscopic study (Thermo Nicolet Nexus 870 spectrophotometer, Madison, Wisconsin, USA) of the jute fiber before and after CR adsorption was done to determine the plausible involvement of functional groups on the fiber surface in the dye-biosorption process. The surface morphology of the jute fiber was investigated before and after CR adsorption with a scanning electron microscope (TESCAN $Vega_{LSV}$, Czech Republic).

Batch Adsorption Studies

Procedure. Batch studies of CR adsorption were performed by contacting washed and oven-dried jute fiber (~ 5 mm length) with 100 mL of CR solution. The mixture was continuously agitated (140 rpm) at 303 K in an incubator for better mass transfer with a high interfacial area of contact. Aliquots were drawn from flasks at regular intervals of times up to 180 min for kinetic study of CR adsorption on the jute fiber. The concentration of CR in the supernatant was estimated with an ultraviolet–visible (UV–vis) spectrophotometer (Perkin Elmer, Lambda 750, Germany) at 497 nm, and the amount of CR adsorbed (q_e; mg/g) by jute fiber from aqueous solution at equilibrium was calculated as follows:[13]

$$q_e = \frac{(C_0 - C_e)V}{m} \quad (1)$$

where C_0 is the initial dye concentration (mg/L), C_e is the equilibrium dye concentration (mg/L), V is the volume of the solution (L), and m is the amount of adsorbent (g). To study the effects of various process parameters, namely, pH (3–12), adsorbent dose (2–10 g/L), C_0 (10–250 mg/L), and temperature (303–323 K), on dye removal, different sets of experiments were conducted with one parameter varied while the others were kept constant. Control experiments with no adsorbent were conducted concurrently to ensure that adsorption occurred by the adsorbent only and not by the container.

Error Analysis. The nonlinear error (χ^2) test was performed for the models as a degree of error between the experimental

and model predicted values. The χ^2 values were calculated as follows:[14]

$$\chi^2 = \sum \frac{(q_e - q_{e,m})^2}{q_{e,m}} \quad (2)$$

where $q_{e,m}$ is the equilibrium adsorption capacity calculated from the model data (mg/g). A small value of χ^2 indicates resemblance between the model data with the experimental values, whereas a large value of χ^2 signifies dissimilarity between them.[14]

Column Adsorption Study

Column Experiments. The behavior of CR removal with the jute fiber in fixed-bed column mode was studied through a series of column experiments with various C_0, F, and Z values. The experimental setup for the continuous-flow column study consisted of a borosilicate glass column (3 cm internal diameter and 30 cm height) with a ceramic sieve (0.5 mm thick) at the bottom to provide support to the bed and also to prevent the washing out of the adsorbent. The column was packed with a known amount of jute fiber to obtain a desired bed height. The top of the bed was covered with a layer of glass wool to prevent the floating up of the jute fiber. A CR solution of known concentration was then percolated through the column at a fixed F. At regular time intervals, samples were collected from the column exit, and concentrations of CR in the collected effluents were analyzed with a UV–vis spectrophotometer (Perkin Elmer, Lambda 750, Germany). The column operation was continued until the CR concentration in the effluent exceeded a value of 99.8% of its C_0. All of the experiments were performed at room temperature (303 ± 3 K) and an initial pH of about 6.2.

Column Performance. The overall performance of a fixed bed column is usually described through the concept of a breakthrough curve. The breakthrough curve is a plot of the relative concentration of the dye solution (ratio of the effluent concentration at any time to C_0) versus the time or volume of the effluent. The breakthrough point is usually defined as the phenomenon when concentration of the effluent is about 3–5% that of the influent.[8] In this study, the breakthrough time (t_b) was considered the time at which the effluent dye concentration (C_t) reached 5 mg/L and the exhaustion time (t_e) was considered when C_t reached 99.8% of C_0. The total mass of adsorbate removed by jute fiber in the column at exhaustion, that is, the maximum capacity of column [total mass of dye adsorbed (m_{ad}; mg)] for a definite C_0 (mg/L) and F (mL/min), could be determined by the calculation of the area under the plot of the adsorbed CR concentration versus effluent time (t; min).[3] Thus, m_{ad} could be computed as follows

$$m_{ad} = \frac{F}{1000} \int_{t=0}^{t=t_{total}} (C_0 - C_t)\,dt \quad (3)$$

where C_0 and C_t are the influent and effluent dye concentrations (mg/L), respectively. The experimental mass of dye adsorbed per unit mass of adsorbent, that is, the experimental adsorption capacity [q_{exp} (mg/g)], was calculated as follows:

$$q_{exp} = \frac{m_{ad}}{\text{Total mass of dry adsorbent in the column (g)}} \quad (4)$$

Modeling of the Column Data. The experimental data of laboratory-scale column studies are the basis of full-scale adsorption column design. Several mathematical models have been developed to analyze laboratory-scale column studies to design pilot-scale columns. In this study, Thomas and bed-depth service time (BDST) models were used to predict the column performance. The Thomas model, which is used to calculate the maximum solid-phase concentration of the solute on the adsorbent and the adsorption rate constant for adsorption in continuous column mode, is as follows:[6]

$$\ln\left(\frac{C_0}{C_t} - 1\right) = \left(\frac{k_{Th} q_{e,Th} M}{F} - k_{Th} C_0 t\right) \quad (5)$$

where $q_{e,Th}$ is the Thomas maximum solid-phase concentration of the solute (mg/g), k_{Th} is the kinetic rate constant of the Thomas model (mL min^{-1} mg^{-1}), and M is the total dry weight of adsorbent in column (g).

The BDST model, the simplest approach for predicting column design and performance, can be given as follows:[5]

$$t_s = \frac{N_o}{C_0 v} Z - \frac{1}{K_a C_0} \ln\left(\frac{C_0}{C_b} - 1\right) \quad (6)$$

where t_s is the service time at the breakthrough point (min), N_o is the adsorption capacity of the bed per unit bed volume (mg/L), Z is the column bed depth (cm), v is the linear velocity (cm/min) and is defined as the ratio of F (mL/min) to the cross-sectional area of bed A (cm^2), C_b is the breakthrough adsorbate concentration (mg/L), and K_a is the rate constant (L mg^{-1} min^{-1}) of the BDST model and characterizes the rate of solute transfer from the liquid phase to the solid phase.

Desorption and Adsorbent Regeneration Studies

For the desorption study, the dye-loaded jute fiber was washed gently with water to remove any unadsorbed dye and dried. The spent adsorbent (1 g) was then agitated (130–140 rpm) at 303 K for 3 h in stoppered Erlenmeyer flasks containing 100 mL of the desorbing agent solution. Four different eluting solvents were used, namely, neutral deionized water, HCl (0.1M), NaOH (0.1M), and CH_3COOH (0.1M). The desorbed CR concentration was quantified with the UV–vis spectrophotometer (Perkin Elmer, Lambda 750, Germany). The desorption efficiency of the adsorbent could be calculated as follows:[15]

$$\text{Desorption efficiency}(\%) = \frac{\text{Amount of dye desorbed from the adsorbent (mg)}}{\text{Amount of dye adsorbed on the adsorbent (mg)}} \times 100 \quad (7)$$

After desorption, the recovered adsorbent was thoroughly washed with deionized water. The regenerated material was then dried and suspended in dye solution to be reused in the next cycle of adsorption experiments. The amount of regenerated adsorbent and other experimental conditions were the same as those used in the aforementioned adsorption studies.

Applied Polymer SCIENCE

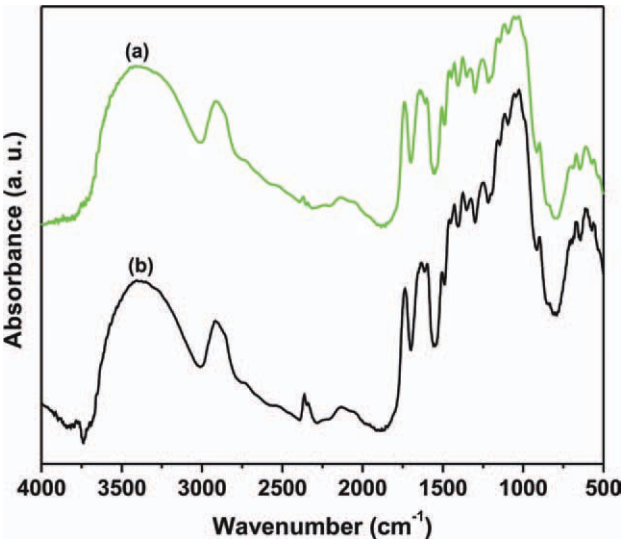

Figure 1. FTIR spectra of the jute fiber (a) before and (b) after dye adsorption. [Color figure can be viewed in the online issue, which is available at wileyonlinelibrary.com.]

RESULTS AND DISCUSSION

Characterization of the Adsorbent

FTIR Study. Figure 1 illustrates the FTIR spectra of the jute fiber before and after CR adsorption. In the FTIR study of both the virgin and CR-adsorbed jute fiber, a characteristic broad band in the range 3200–3600-cm^{-1} was observed for hydrogen-bonded —OH stretching. The peaks at 2910 cm^{-1} represented the —CH stretching vibration of methyl and methylene groups in cellulose and hemicellulose. The absorbance bands at 1452, 1374, and 1035 cm^{-1} were ascribed to —CH_3 asymmetric stretching, —CH symmetric stretching, and aromatic —CH in-plane deformation in lignin, respectively. The band at 1738 cm^{-1} represented C—O stretching of the carboxyl and ester groups in the hemicelluloses of the fiber. The peak at 1249 cm^{-1} corresponded to C—O stretching in the acetyl groups in hemicellulose.[16] The absorbance maximum ratio of the —OH group (3380 cm^{-1}) to the internal standard peak (2920 cm^{-1}) of the methyl and methylene groups of the jute fiber was found to decrease from 1.2535 to 1.1399 after adsorption. This indicated the involvement of —OH groups in the CR adsorption.

Scanning Electron Microscopy (SEM) Analysis. The surface morphology of the jute fiber before and after CR adsorption is presented in Figure 2. The SEM micrograph of the pristine jute fiber [Figure 2(a)] showed that the surface of the jute fiber was smooth, but an uneven and irregular surface morphology was observed in case of the CR-adsorbed jute fiber [Figure 2(b)]. It was also observed that the natural golden color of the jute fiber became red after the adsorption process; this clearly indicated that the surface of the fiber was covered with the dye molecules [Figure 2(c,d)].

Batch Adsorption Study

Effect of pH on adsorption. The effect of the initial pH on the adsorption of CR from its aqueous solution by jute fiber is shown in Figure 3(a). This figure shows that the dye removal increased as the initial pH of the solution increased from 3 to 4 but decreased drastically as the pH increased further from 4 to 12. The adsorptive process was affected by the change in solution pH because of the protonation and deprotonation of active functional groups of the adsorbent and adsorbate.[17] The lower adsorption at pH 3 was due to the interionic repulsion between the positively charged dye molecules and the adsorbent. At pH 4, the nitrogen atoms and sulfonate groups of the dye molecules became protonated (=N^+—, i.e., positively charged, and —SO_3H, i.e., neutral, respectively),[18] whereas at pH 3.6, the surface charge of the adsorbent remained negative because the point of zero charge (pH_{PZC}) of the jute fiber was approximately 3.6 (see Supporting Information, Figure S2), which resulted in an electrostatic attraction between the positively charged dye molecules and the negatively charged adsorbent, which in turn, led to the maximum removal of CR (86%) by jute fiber at pH 4. On the contrary, as pH was increased from 4 to 12, the negative surface charge of the jute fiber hindered the adsorption of CR by electrostatic repulsion between the deprotonated dye molecules and the negatively charged jute fiber. Consequently, the dye removal decreased to 50.8%.

Effects of the contact time and initial dye concentration of the solution on adsorption. The results of the experiments conducted to evaluate the contact time needed by the systems to reach equilibrium and the influence of initial dye concentration are presented in Figure 3(b). The dye adsorption increased with increasing contact time and finally attained an apparent equilibrium after 25–35 min, depending on the C_0 of the solution. The dye uptake in the initial phase of contact time was very rapid, and 80% adsorption was completed within 25 min; this was followed by a gradual removal of dye, which continued for a longer period. The rapid adsorption during the initial stage was probably due to the abundant availability of active sites on the sorbent surface. At this stage, the adsorption mainly took place on the surface of the adsorbent. After the rapid dye uptake at the very beginning, the adsorbent became exhausted because of the gradual occupancy of the active sites, and the adsorption was replaced by the transportation of dye from the external sites to the internal sites of the adsorbent particles. Thus, the uptake rate began to decline.[19]

It can be observed from Figure 3(b) that q_e of the jute fiber for CR increased from 2.8 to 9.0 with increasing C_0 from 10 to 250 mg/L; this indicated a dependency of the dye removal on C_0. As the dye concentration in aqueous solution increased, more dye molecules became available for adsorption on the adsorbent surface. This was probably due to the effect of the concentration gradient between dye in solution and dye on the jute fiber surface at higher dye concentrations, which produced the main driving force for mass transfer during the adsorption process.[20] However, the dye-removal percentage at equilibrium decreased from 85 to 30 as C_0 increased from 10 to 250 mg/L. This phenomenon was due to the fact that at lower concentration, the ratio of the initial number of dye molecules to the available surface area was low, and subsequently, the fractional adsorption became independent of C_0. However, at higher concentrations, the available sites of adsorption became limited, and hence, the percentage removal of dye was dependent on C_0.[21]

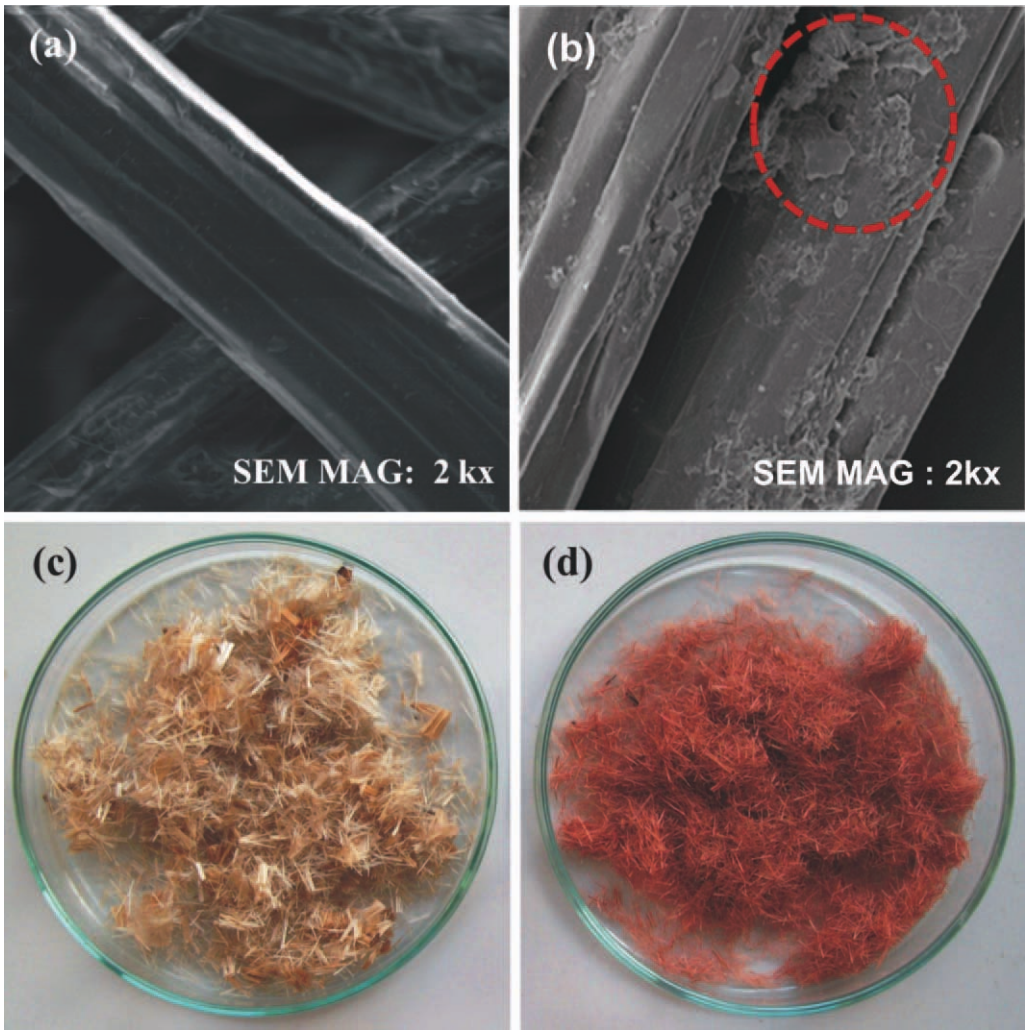

Figure 2. SEM images of the (a) pristine and (b) dye-adsorbed jute fiber. Photographs of the (c) pristine and (d) dye-adsorbed jute fiber. [Color figure can be viewed in the online issue, which is available at wileyonlinelibrary.com.]

Effect of adsorbent dosage on adsorption. Figure 3(c) represents the effect of the adsorbent dosage on the adsorption capacity of the jute fiber for CR. The adsorption capacity of jute fiber decreased at higher adsorbent dosages because of the significant unsaturation of adsorption sites at the constant dye concentration and volume.[22] The effective utilization of active sites was caused by the establishment of better contacts between the adsorbent particles and dye molecules with a small amount of adsorbent; that is, a low adsorbent-to-adsorbate ratio increased the adsorption capacity at lower adsorbent dosages.[23] However, the removal of CR increased from 17.89 to 55.74%, with increasing amount of jute fiber from 2 to 10 g/L. This may have been due to the greater availability of surface area and an increase in the number of adsorption sites of the adsorbent with increasing amount of adsorbent.[24]

Effect of the ionic strength of the solution on dye removal. Sodium salt is often used as a stimulator in the dye industry, and sodium dodecyl sulfate (SDS), an anionic surfactant, is often present in the effluent of dye industries. The presence of these salts affect the ionic strength of the solution, which in turn, influences the adsorption process, as it changes the activity coefficients of OH^-, H_3O^+ and, specifically, electrolyte ions by controlling the extent of the electric double layer around the adsorbent particles and affecting the electrostatic forces between the adsorbent and the charged species.[25] Hence, the effect of the addition of these salts in small quantities on the adsorption of CR by the jute fiber was investigated. As shown in Figure 3(d), an increase in the ionic strength of the solution with the addition of NaCl and SDS significantly increased the extent of adsorption. The removal of CR increased from 51.4 to 99.9% with increasing concentration of NaCl from 0 to 1.5*M*. Moreover, the addition of SDS (3%) enhanced the removal of CR to 57.5%. When the solution pH was 6.2 (pH at which the effect of the ionic strength on dye adsorption was studied), both the jute fiber surface and the dye molecules became negatively charged, as the pH_{PZC} of jute fiber was approximately 3.6 and the pK_a of CR was 4.5–5.5.[18] Theoretically, when the surface charge of the adsorbate and adsorbent are opposite, that is, the electrostatic forces between the adsorbent surface and adsorbate molecules are attractive, an increase in the ionic strength will decrease the removal of adsorbate.

Applied Polymer SCIENCE

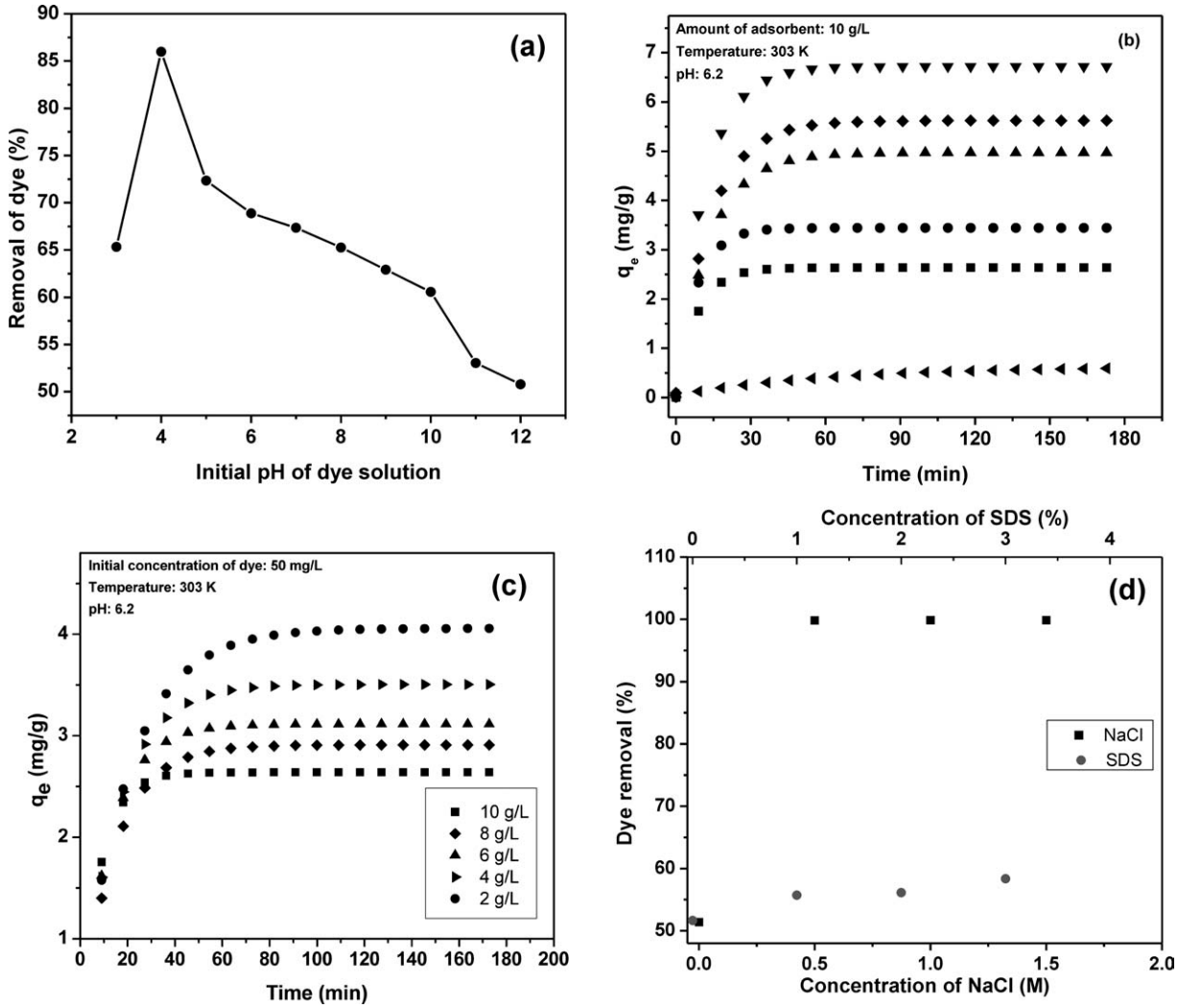

Figure 3. Effects of (a) pH, (b) *m*, (c) C_0 [(◀) 10, (■) 50, (●) 100, (▲) 150, (◆) 200, and (▼) 250 mg/L], and (d) ionic strength of the dye solution on CR adsorption by the jute fiber.

Conversely, when the surface charge of both the adsorbate and adsorbent are identical, that is, the electrostatic forces between them are repulsive, as in this case, an increase in the ionic strength will increase the adsorption.[18] The experimental results obtained from this investigation show an enhancement in dye adsorption with an increase in the ionic strength of the solution. The adsorption of negatively charged dye molecules on the negatively charged jute fiber increased with salt addition because of the decrement of negative charge on the adsorbent surface with increasing ionic strength; this increased the electrostatic interaction between the dye and adsorbent. Similar observations were also reported by Hu et al.[25] for the adsorption of CR by cattail root.

Effect of the temperature on dye adsorption. Various textile dye effluents are usually discharged at relatively higher temperatures. Hence, the effect of the temperature on the biosorption process of the dye by the jute fiber was studied as a vital factor.[11] From Figure 4(a), it can be perceived that the temperature adversely affected the removal efficacy of the jute fiber for CR. The adsorption capacity of the jute fiber decreased from 2.818 to 1.984 mg/g as the temperature increased from 303 to 323 K. The reason behind the drop in the adsorption efficiency at elevated temperatures could be explained by the following facts:[23,25]

1. At higher temperatures, the mobility of the solute molecules increased. Consequently, the solute molecules showed an inclination to escape from the solid phase and reentered the liquid phase. This resulted in a reduction of the adsorption capacity of the jute fiber.
2. At elevated temperatures, the interaction between the active sites of the adsorbent and dye molecules weakened due to the weakening of physical forces, such as hydrogen bonds and van der Waals interaction. As a result, the amount of dye molecules held by the adsorbent decreased.
3. As the temperature was increased, the pores of the adsorbent expanded, and some of the dye molecules from the adsorbent were released into the aqueous solution. This led to a decrease in the removal percentage of the dye.

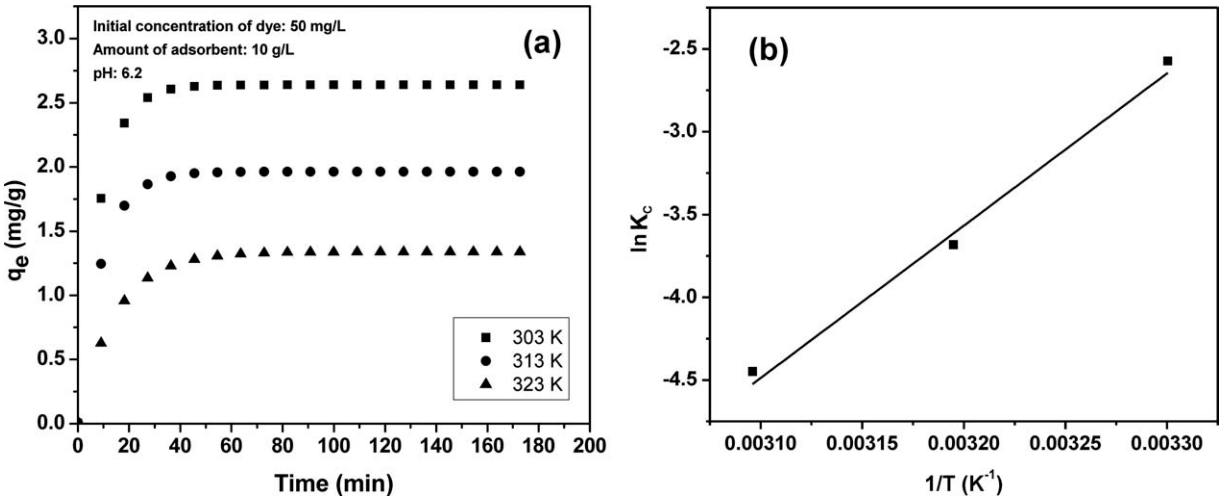

Figure 4. (a) Effect of the temperature on the dye adsorption by jute fiber. (b) Plot for ln K_C versus $1/T$ for the CR adsorption onto the jute fiber.

The higher adsorption capacity at lower temperatures implied that the biosorption process of CR by the jute fiber was exothermic in nature.

Calculation of the Thermodynamic Parameters. Thermodynamic parameters were calculated to evaluate the thermodynamic feasibility of the adsorption process and to confirm the nature of the adsorption process with the following relation:[25]

$$\Delta G^o = \Delta H^o - T\Delta S^o \tag{8}$$

We also used the van 't Hoff equation as follows:

$$\ln K_C = \frac{\Delta S^o}{R} - \frac{\Delta H^o}{RT} \tag{9}$$

where ΔG^0 is the change in the Gibbs free energy (kJ mol^{-1}), ΔH^0 is the change in enthalpy (kJ/mol), ΔS^0 is the change in entropy (J mol^{-1} K^{-1}) of adsorption, T is the adsorption temperature (K), R is the universal gas constant (8.314 J/mol/K), and K_C is the distribution coefficient for the adsorption process, which is the ratio of the equilibrium concentration of the dye ions attached to the jute fiber compared to the equilibrium concentration of the dye ions in the aqueous phase. The values of ΔH^0 and ΔS^0 were calculated from the slope and intercept of the linear plots of ln K_C versus $1/T$ [Figure 4(b)]. Once these two parameters were obtained, ΔG^0 was determined from eq. (8). Theoretically, it was expected that the adsorption processes (either from gas or liquid phase) would be exothermic because of the liberation of heat during bond formation between the solute and adsorbent.[18] The negative value of ΔH^0 (−33.14 kJ/mol) confirmed the exothermic nature of CR adsorption by the jute fiber. The values of ΔG^0 at 303, 313, and 323 K were −24.53, −24.25, and −23.97 kJ/mol, respectively. The negative values of ΔG^0 demonstrated the thermodynamic feasibility and spontaneity of the adsorption process. The shifting of ΔG^0 to higher negative values with decreasing temperature indicated that the studied adsorption was rapid and more favorable at lower temperatures with a higher affinity of CR onto the jute fiber.[25] The adsorption was associated with a negative value of ΔS^0 (−28.39 J mol^{-1} K^{-1}); this revealed the decreased randomness of dye molecules at the solid–solution interface, and no significant changes occurred in the internal structure of adsorbent during dye fixation on the active sites of the jute fiber. Similar observations were also reported by Vimonses et al.[14] for CR adsorption by Australian clay.

Adsorption Isotherms. Adsorption isotherm models are fundamental for estimating the adsorption capacity of adsorbent for designing an operating adsorption system for industrial effluents. The experimental data of dye adsorption onto the jute fiber were analyzed by two well-known adsorption isotherm models, the Langmuir and Freundlich models.

Langmuir isotherm. The Langmuir adsorption isotherm assumes that the adsorption occurs with a monolayer coverage of adsorbate onto a homogeneous adsorbent surface. The linearized and rearranged form of the Langmuir equation [eq. (10)] is as follows:[26]

$$\frac{1}{q_e} = \left(\frac{1}{bq_m}\right)\frac{1}{C_e} + \frac{1}{q_m} \tag{10}$$

where q_m is the mass of adsorbed solute required for complete saturation of a unit mass of adsorbent, that is, the maximum monolayer capacity of the adsorbent (mg/g), and b is the Langmuir constant (L/mg), which represents the energy or net enthalpy of the adsorption process.

q_m and b were computed from the slopes and intercepts of the straight line obtained from the linearized plot of $1/q_e$ versus $1/C_e$ [Figure 5(a)]. The adsorption of CR onto the jute fiber fit very well with the Langmuir model and had a correlation coefficient of 0.999 and small χ^2 value. This demonstrated the monolayer coverage of CR onto the jute fiber (Table I). The theoretical maximum monolayer adsorption capacity of the jute fiber for CR was calculated to be 8.12 mg/g. The calculated maximum q_m was found to be very close to q_e from the experiment. Thus, the Langmuir isotherm model described the experimental data of the adsorption of CR by the jute fiber precisely.

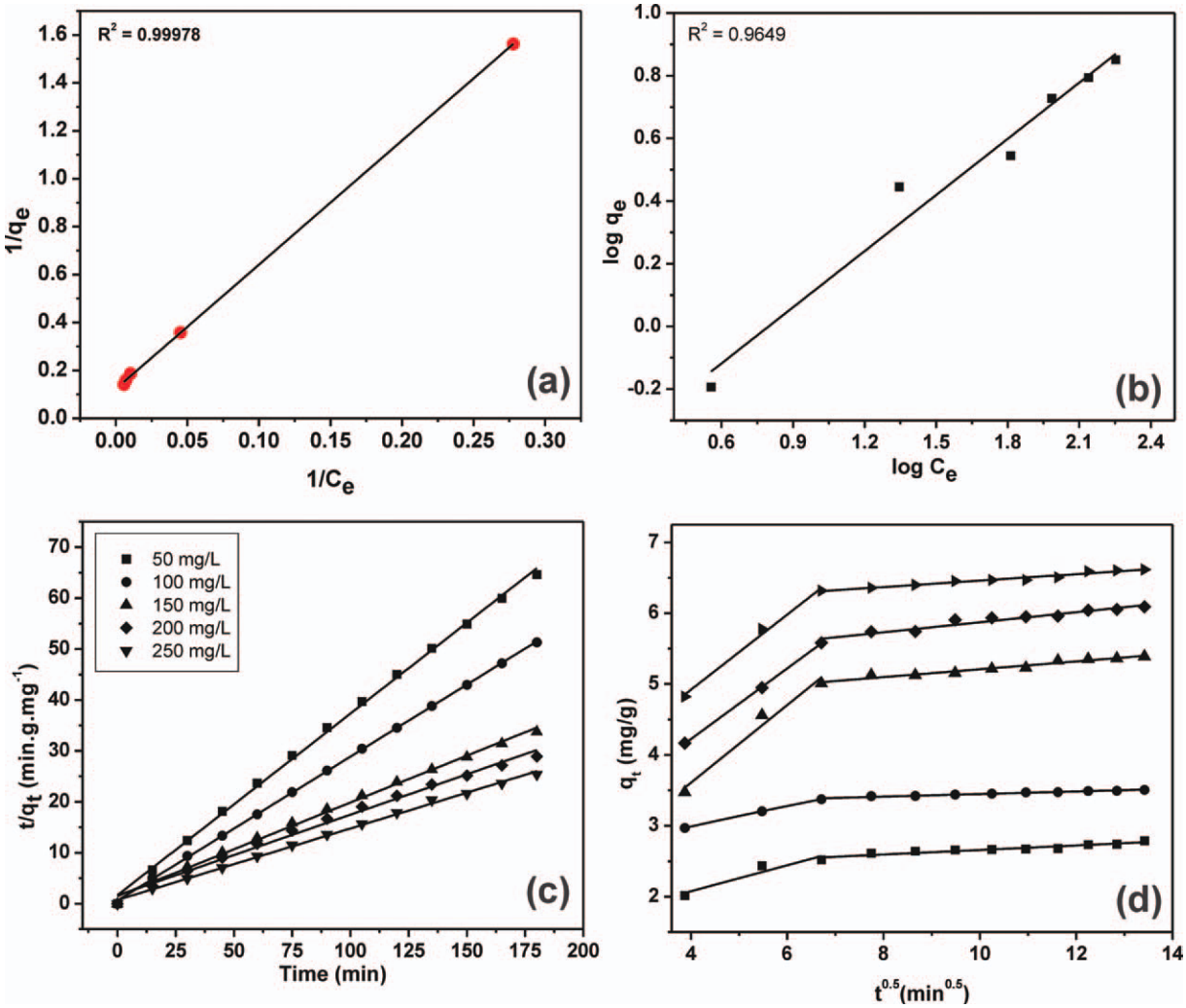

Figure 5. (a) Langmuir and (b) Freundlich isotherm, (c) pseudo-second-order kinetic, and (d) intraparticle diffusion model [(■) 50, (●) 100, (▲) 150, (◆) 200, and (▼) 250 mg/L] plots for CR adsorption onto the jute fiber. [Color figure can be viewed in the online issue, which is available at wileyonlinelibrary.com.]

Calculation of the Dimensionless Separation Factor (R_L). The essential feature of the Langmuir adsorption isotherm could be expressed in terms of a dimensionless constant separation factor or equilibrium parameter (R_L) with the Langmuir isotherm parameter. The following equation defines R_L:[26]

$$R_L = \frac{1}{1 + bC_o} \tag{11}$$

When R_L is greater than unity and equal to one, the process is supposed to be unfavorable and linear, respectively. Meanwhile,

Table I. Isotherm Parameters and separation factors for the Adsorption of CR onto the Jute Fiber

Isotherm model parameters									
		Langmuir isotherm				Freundlich isotherm			
Temperature (K)	q_e (mg/g)	q_m (mg/g)	b (L/mg)	R^2	χ^2	K (mg/g)	$1/n$	R^2	χ^2
303	7.382	8.116	0.2378	0.9998	0.1507	2.993	0.597	0.9648	16.9851
R_L values at different initial dye concentrations									
Temperature (K)	C_0 (mg/L)								
	10	50	100	150	200	250			
303	0.2960	0.0776	0.0404	0.0273	0.0206	0.0165			

Table II. Kinetic Parameters for the Adsorption of CR onto the Jute Fiber at Different initial dye concentrations (mg/L)

		C_0 (mg/L)				
Kinetic model	Model parameter	50	100	150	200	250
Pseudo-first-order	$q_{e,exp}$ (mg/L)	2.818	3.507	5.390	6.227	7.382
	$q_{e,cal}$ (mg/L)	1.471	1.909	2.217	2.759	1.879
	k_1 (g mg^{-1} min^{-1})	0.0368	0.0467	0.0416	0.0345	0.0352
	R^2	0.9584	0.9555	0.9693	0.9196	0.8847
	χ^2	3.353	1.337	11.452	13.357	12.653
Pseudo-second-order	$q_{e,cal}$ (mg/L)	2.804	3.536	5.441	6.305	7.123
	k_2 (g mg^{-1} min^{-1})	0.1341	0.0763	0.0272	0.0169	0.0156
	R^2	0.9998	0.9999	0.9997	0.9984	0.9989
	χ^2	0.001	0.002	0.002	0.002	0.001
Intraparticle diffusion	k_{id1} (mg g^{-1} min$^{-0.5}$)	0.1432	0.1828	0.4989	0.5304	0.5487
	k_{id2} (mg g^{-1} min$^{-0.5}$)	0.0166	0.0275	0.0534	0.0630	0.0462
	I_{id1}	1.9851	2.9193	3.3242	3.9713	4.6540
	I_{id2}	2.3906	3.2838	4.6781	5.2548	5.9968
	R^2	0.9993	0.9827	0.9995	0.9862	0.9497
Liquid-film diffusion	k_{fd} (min^{-1}) $\times$ 10^{-3}	−16.02	−23.01	−18.09	−15.00	−15.26
	I_{fd}	−1.411	−1.901	−0.877	−0.813	−1.328
	R^2	0.9584	0.9555	0.9694	0.9196	0.8848

an irreversible process takes place when the value of R_L is calculated to be zero. Favorable conditions occur only when the R_L values are within the range $0 < R_L < 1$.[26] The R_L values calculated in the study of C_0 values were determined to be 0.296–0.0165, that is, well within the defined range. This suggests that the adsorption of dye onto the jute fiber was a favorable process under the conditions used for these experiments (Table I).

Freundlich isotherm. The Freundlich model, the earliest known empirical relationship for describing adsorption equilibrium, illustrates the heterogeneity of the adsorbate surface, and the linearized form of the equation is given by

$$\log q_e = \log K_F + \frac{1}{n}\log C_e \tag{12}$$

where K_F is an empirical constant (mg/g) signifying the adsorption capacity and n, also a constant, is the heterogeneity factor, which is indicative of the bond energies between the dye and the adsorbent.[11]

The graphical presentation of the Freundlich isotherm model is expressed in Figure 5(b). The model parameters and error functions reflected that this isotherm model showed poorer fit to the experimental data (correlation coefficient = 0.9648) than the Langmuir isotherm under the studied C_0's (Table I).

Adsorption Kinetics. The prediction of the adsorption mechanism and its potential rate-controlling steps is an important issue to be considered. The adsorption dynamics of CR onto the jute fiber were investigated with kinetic models, namely, the pseudo-first-order, pseudo-second-order, intraparticle diffusion, and liquid-film diffusion models.[22]

Pseudo-first-order model. The linearized form of the pseudo-first-order rate equation was given by[27]

$$\log(q_e - q_t) = \log q_e - \frac{k_1}{2.303}t \tag{13}$$

where q_t is the amount of adsorbed CR at time t (mg/g), k_1 is the rate constant of pseudo-first-order adsorption (min^{-1}), and t is the contact time. The linear plot of $\log(q_e - q_t)$ versus t (figure not shown) provided a poor R^2 value, a large χ^2 value, and a high disparity between the experimental adsorption capacity and the calculated one (Table II). This indicated that the first-order-model had very limited applicability to the adsorption kinetics of CR onto the jute fiber.[22]

Pseudo-second-order model. The linear form of the pseudo-second-order kinetic model is expressed as follows:[27]

$$\frac{t}{q_t} = \frac{1}{k_2 q_e^2} + \frac{1}{q_e}t \tag{14}$$

where k_2 (g mg^{-1} min^{-1}) is the rate constant of second-order adsorption. When the experimental data for the studied range of C_0's were analyzed by the pseudo-second-order model, the straight lines obtained through the plot of t/q_t versus t [Figure 5(c)] generated R^2 values close to 1 and negligible χ^2 values (Table II). A comparison of the error functions suggested that the pseudo-second-order kinetic model provided a better fit to the experimental data for the adsorption of CR onto the jute fiber than the pseudo-first-order model. The calculated adsorption capacity ($q_{e,cal}$) was quite agreeable with that obtained from the experimental findings; this confirmed the applicability of the pseudo-second-order equation to the adsorption process

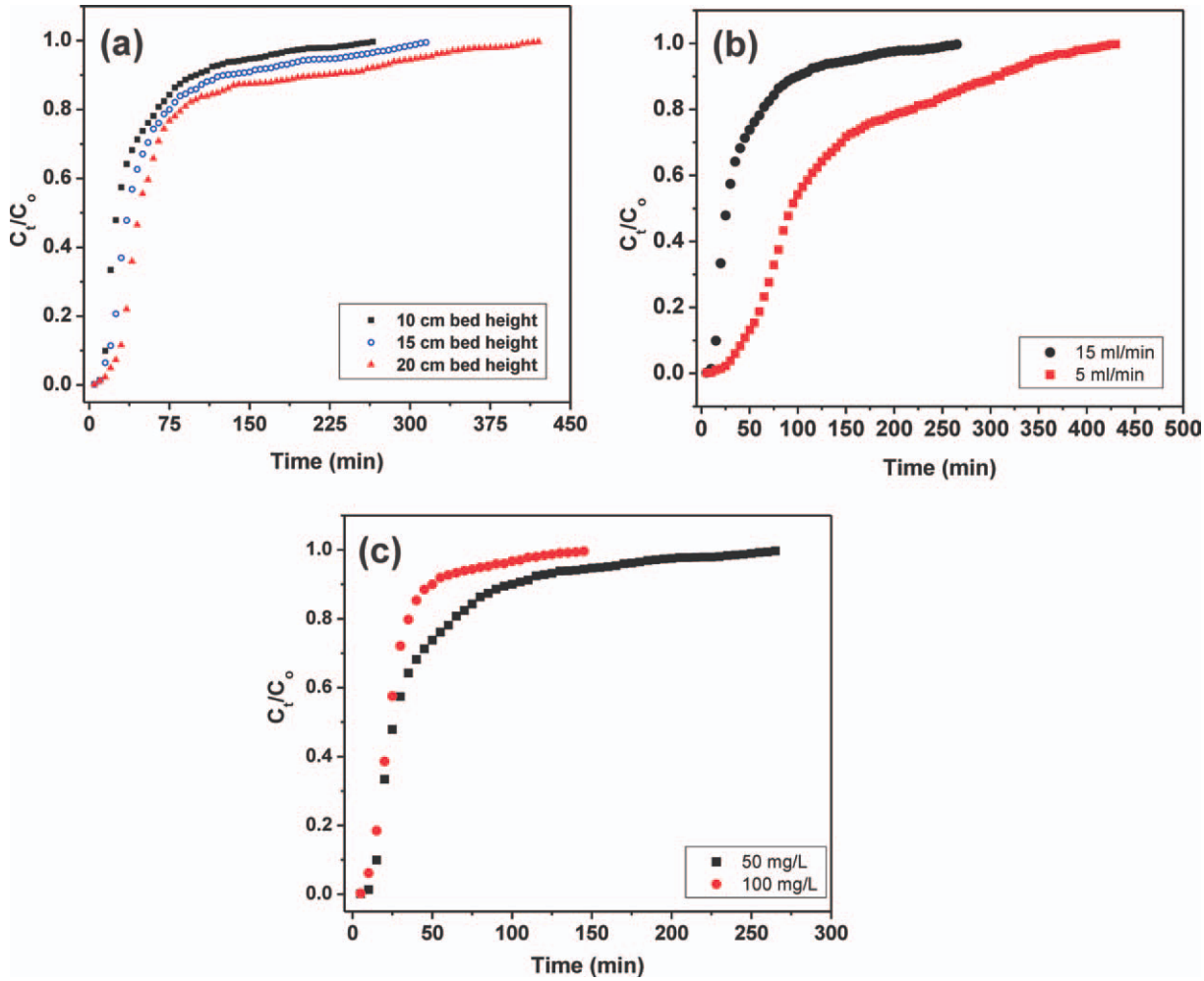

Figure 6. Breakthrough curves for CR adsorption onto the jute fiber at different (a) bed height, (b) *F*, and (c) C_0 values. [Color figure can be viewed in the online issue, which is available at wileyonlinelibrary.com.]

(Table II). The computed parameters and error functions from the pseudo-second-order kinetic model also indicated that for the studied cases and conditions, the adsorption kinetics of CR onto jute fiber could be accurately described by this model.[27]

Intraparticle diffusion model. In this study, the possibility of intraparticle diffusion in the kinetic process was investigated with the following equation:

$$q_t = k_{id} t^{0.5} \tag{15}$$

where k_{id} is the equilibrium rate constant of intraparticle diffusion (mg g^{-1} $min^{-0.5}$).[22] The intercepts (I_{id}) of the plots q_t against $t^{0.5}$ from the intraparticle diffusion model give the measurement of the boundary layer thickness. The multilinearity of the plots [Figure 5(d)] implied that more than one mode of adsorption was involved in the uptake of CR by the jute fiber, and this indicated the complexity of the process. The short initial linear portion in Figure 5(d) shows the external mass transfer, in which the adsorbate migrated through the solution to the external surface of the adsorbent via macropore diffusion during the early stage of adsorption. On the other hand, the long successive linear portion may have been due to the gradual adsorption stage with intraparticle diffusion via micropores.[19]

Liquid-film diffusion model. Assuming that liquid-film diffusion may contributed to the determination of adsorption, the kinetic data were analyzed by the liquid-film diffusion model, given as follows:

$$\ln(1 - F) = -k_{fd} t \tag{16}$$

where $F = q_t/q_e$, that is, *F* is the fraction of solute adsorbed at different times and k_{fd} is the liquid-film diffusion rate constant (min^{-1}). The plots of $\ln(1 - F)$ versus *t* (figure not shown) were linear, having R^2 and intercept (I_{fd}) values within the ranges 0.9694–0.8848 and −15.00 to −23.01, respectively (Table II). The deviation of the straight lines from the origin in the plots suggested that the liquid-film diffusion model did not describe this adsorption system accurately.[28]

Effect of Various Parameters on the Column Performance

The effects of bed height, flow rate, and initial dye concentration were studied for the adsorption of CR by the jute fiber in

Table III. Effects of Different Bed Heights, flow rates, and initial dye concentration on the Column Parameters

Z (cm)	F (mL/min)	C_0 (mg/L)	t_b (min)	t_e (min)	m_{ad} (mg)	$q_{e,exp}$ (mg/g)
10	15	50	15	265	30.12	2.008
15	15	50	18	315	41.014	2.051
20	15	50	28	420	56.225	2.249
10	5	50	45	430	32.19	2.146
10	15	100	7	145	36.03	2.402

column mode. The breakthrough curves of dye adsorption at different conditions of column operation were expressed plots of C_t/C_0 versus t.

Effect of the Bed Depth. The effect of the bed height on the column performance was studied with 10, 15, and 20 cm bed depths; these were obtained when the column was packed with 15, 20, and 25 g of jute fiber, respectively. Figure 6(a) shows the adsorption breakthrough curves for different bed depths at $F = 15$ mL/min and $C_0 = 50$ mg/L, yielded by plotting C_t/C_0 versus t. It can be observed from Table III, that as the bed height in the column increased, m_{ad} at exhaustion time increased. The maximum bed capacity (q_e) was achieved at the highest bed height. This was due to the fact that as the column bed height increased, the surface area of the adsorbent increased because of the increasing adsorption dose, which in turn, increased the adsorption sites for CR on the jute fiber. As the bed depth increased, the contact time of influent inside the column increased; this permitted a deeper diffusion of adsorbate molecules into the adsorbent.[4] Thus, when Z was increased from 10 to 20 cm, t_b and t_e increased from 15 to 28 min and 265 to 420 min, respectively.

Effect of flow rate. The investigation of the effect of flow rate on the performance of the column (the bed height and C_0 were 10 cm and 50 mg/L, respectively) was executed with different F values: 5 and 15 mL/min. Figure 6(b) shows the respective breakthrough profiles. The values of t_b and t_e decreased from 45 to 15 min and 430 to 265 min, respectively, as F was increased from 5 to 15 mL/min. The reason behind this phenomenon was the fact that at higher F values, the residence time of CR in the column was insufficient to establish an adsorption equilibrium, and hence, the adsorbate exited the column before equilibrium was reached. Thus, at higher F values,the intraparticle diffusion of the dye decreased, and the mass transfer rate increased. This led to faster column saturation.[8] This, in turn, resulted in a significant decrease in the dye adsorption capacity (Table III).

Effect of initial dye concentration. Initial dye concentration had a significant effect on column performance. Figure 6(c) shows the breakthrough curves obtained for different C_0's (50 and 100 mg/L) at $F = 15$ mL/min and column depth = 10 cm and implies that better column performance could be achieved at lower C_0's. With an increase in C_0 from 50 to 100 mg/L, t_b decreased from 15 to 7 min. t_e was also significantly affected by C_0. The t_e values for C_0 values of 50 and 100 mg/L were 265 min (corresponding to a 3975-mL throughput volume) and 145 min (corresponding to a 390-mL throughput volume), respectively. At a higher inlet concentration, faster transport, caused by the higher concentration gradient due to an increased diffusion coefficient and also a quick saturation of adsorption sites, resulted in decreases in t_e and throughput volume.[3] The m_{ad} values at t_e and q_e increased with increasing C_0 (Table III) because of the high driving force for the adsorption process provided by the high concentration difference.[4]

Table IV. Thomas Model Parameters Calculated with Linear Regression Analysis under Different Conditions

Z (cm)	F (mL/min)	C_0 (mg/L)	k_{Th} (mL mg^{-1} min^{-1})	$q_{e,exp}$ (mg/g)	$q_{e,cal}$ (mg/g)	R^2
10	15	50	0.320	2.1218	2.008	0.9709
15	15	50	0.216	2.3510	2.051	0.9384
20	15	50	0.160	2.5204	2.249	0.9360
10	5	50	0.214	2.4002	2.146	0.9634
10	15	100	0.307	2.6554	2.402	0.9675

Modeling of the Column Data

Thomas Model. The experimental data obtained from the column operation for CR adsorption onto the jute fiber were subjected to the Thomas model. The data at C_t/C_0 values higher than 0.05 and lower than 0.98 for all sets of column studies were considered for modeling. The Thomas rate constant (k_{Th}) and maximum solid-phase concentration (q_e) were computed from the slope and intercepts, using linear regression.[8] The Thomas model parameters are presented in Table IV. R^2 values ranging from 0.93 to 0.97, evaluated from regression coefficient analysis, indicated that the regressed lines provided excellent fits to the experimental data treated with the Thomas model. As the F value of the operating column increased, the bed capacity (q_e) decreased, but the rate constant (k_{Th}) increased. Conversely, with increasing C_0 and bed height, the value of q_e increased, and the value of k_{Th} decreased. Thus, better column performance could be achieved with lower flow rates, higher bed heights, and lower initial dye concentration.

BDST Model. The capability of the BDST model to predict the column performance was inspected with the experimental data obtained from column operation. The constants N_o and K_a were calculated from t_s versus Z plots for C_t/C_0 values of 0.2, 0.6, and 0.9. A consistent increase in the slope from 1.7 to 12.04 min/cm with increasing C_t/C_0 and successive increases in the corresponding N_o from 180.23 to 1279.08 mg/L can be observed in Table V. The lower adsorption capacity at low breakthrough

Table V. BDST Model Parameters for the Adsorption of CR at C_0 = 50 mg/L and F = 15 mL/min

C_t/C_0	a (min/cm)	b (min)	K_a (L mg^{-1} min^{-1})	N_o (mg/L)	R^2
0.2	1.6979	0.3510	0.07899	180.2321	0.9864
0.6	2.3044	−8.3390	0.00097	244.6120	0.9981
0.9	12.0498	−24.1923	0.00182	1279.0862	0.9832

than that at exhausted conditions of the column bed was due to the unsaturation of several adsorbent active sites by the dye molecules. However, as the value of C_t/C_0 increased, the K_a value decreased. The high R^2 values (>0.98) demonstrated the validity of the BDST model for this system.

Batch Desorption and Adsorbent Regeneration Studies

The desorption studies of the dye-adsorbed jute fiber gave an important insight into the overall adsorption mechanism. A very low desorption (2.6%) of CR was obtained with 0.1*M* HCl, whereas water and 0.1*M* CH_3COOH desorbed 24.5 and 14.8% of the dye, respectively. The maximum desorption of dye (82.3%) was achieved by 0.1*M* NaOH; this indicated that the dye molecules were attached to the adsorbent, most probably by ion exchange.[24]

The adsorption efficiency of the jute fiber deteriorated during the adsorption–desorption cycles of CR onto the jute fiber. The adsorption of dye diminished slightly from 55.78 to 52.60% in the first reused cycle and then further decreased to 48.06, 45.31, and 43.21% in the second, third, and fourth cycles, respectively.

Adsorption Mechanism

In an adsorption study, the proposition of the mechanism is the foremost challenge. The structure of the adsorbate and the properties of an adsorbent surface having various functional groups must be taken into account to elucidate the adsorption mechanism. In this context, it is necessary to mention that CR was an anionic dye containing amine, sulfonate, and azo groups as functional groups, whereas the FTIR study (Figure 1) confirmed the major presence of oxygen-containing functional groups, such as hydroxyls, ethers, and carbonyls, in the jute fiber.[16] Combining the experimental findings of this study and FTIR analyses and considering the structure of the adsorbate and adsorbent, we assumed that the mechanism for CR adsorption by the jute fiber included the involvement of physical forces, such as hydrogen bonding between N, S, O, and the benzene ring of CR and —OH groups of the jute fiber surface, and van der Waals forces, during the adsorption process. Figure 7 represents a plausible mechanism of anionic dye adsorption by the jute fiber.[29] The desorption study in batch mode suggested that ion exchange may also be a possible mechanism of dye adsorption onto the jute fiber.

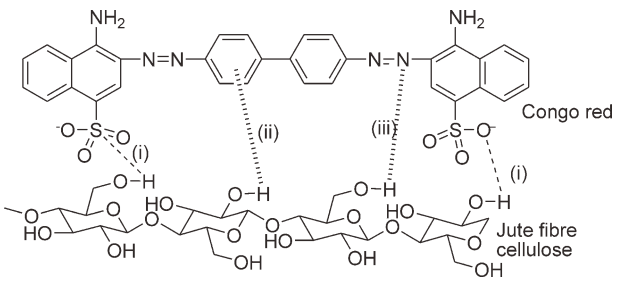

Figure 7. Schematic representation of the CR–jute fiber cellulose unit interaction: (i) hydrogen bonding between the hydroxyl group of the jute fiber and electronegative atoms of the dye molecule, (ii) Yosida H bonding between the hydroxyl group of jute fiber and the aromatic residue in the dye, and (iii) hydrogen bonding between the hydroxyl group of the jute fiber and the azo group of the dye.

Table VI. Comparison of the Langmuir Adsorption Capacity of the Jute Fiber with Other Low-Cost Unmodified Adsorbents for Azo Dye Removal

Adsorbent	Dye	Adsorption capacity (mg/g)	Reference
Cashew nut shell	CR	5.18	13
Australian kaolin	CR	7.27	14
Activated carbon of *Thespesia populnea* pods	Orange G	9.13	30
Sugarcane bagasse	Methyl red	5.66	31
Mango seed	Acid orange 10	8.3	32
Kaolin	CR	5.44	33
Untreated jute fiber	CR	8.12	This study

However, we believe that more experiments are needed to confirm this proposed mechanism.

CONCLUSIONS

The maximum removal of dye was observed at pH 4 in the batch adsorption study. The adsorption of dye increased with increasing adsorbent dosage and ionic strength of solution and decreased as C_0 increased. The spontaneity and exothermic nature of the process was confirmed by the negative ΔG^0 values and positive ΔH^0 values obtained from the thermodynamic study. The adsorption process agreed reasonably well with the Langmuir equilibrium isotherm and pseudo-second-order kinetic model, with $R^2 = 0.999$. Fast dye adsorption and quick attainment of equilibrium is desirable and advantageous for practical applications. The experimental column data revealed that both t_b and t_e increased with increasing bed height. However, increases in F and C_0 decreased t_b and t_e, which resulted in faster saturation of the column. Both the Thomas and BDST models successfully described the adsorption of CR onto the jute fiber in column mode with various experimental conditions. Although a direct comparison of the adsorption capacity of the jute fiber with other low-cost adsorbents was difficult because of the employment of nonidentical experimental conditions, it can be observed from Table VI that the adsorption capacity of the jute fiber for azo dye adsorption was reasonably good and comparable to other adsorbents. Thus, the batch and column adsorption studies identified jute fiber as an alternative, efficient and inexpensive adsorbent for treating dye-contaminated wastewater. After observing significant performance with untreated jute fibers for dye removal, our research group is currently involved in further improving the performance with suitable chemical modification.

REFERENCES

1. Zhang, W.; Yan, H.; Li, H.; Jiang, Z.; Dong, L.; Kan, X.; Yang, H.; Li, A.; Cheng, R. *Chem. Eng. J.* **2011,** *168*, 1120.
2. Goshadrou, A.; Moheb, A. *Desalination* **2011,** *269*, 170.
3. Han, R.; Wang, Y.; Zhao, X.; Wang, Y.; Xie, F.; Cheng, J.; Tang, M. *Desalination* **2009,** *245*, 284.

4. Han, R.; Ding, D.; Xu, Y.; Zou, W.; Wang, Y.; Li, Y.; Zou, L. *Bioresour. Technol.* **2008,** *99*, 2938.
5. Zambrano, J. B.; Szygula, A.; Ruiz, M.; Sastre, A. M.; Guibal, E. *J. Environ. Manage.* **2010,** *91*, 2669.
6. Song, J.; Zou, W.; Bian, Y.; Su, F.; Han, R. *Desalination* **2011,** *265*, 119.
7. Afkhami, A.; Moosavi, R. *J. Hazard. Mater.* **2010,** *174*, 398.
8. Uddin, T.; Khan, R.; Islam, M. R. A. *J. Environ. Manage.* **2009,** *90*, 3443.
9. Valderrama, C.; Arévalo, J. A.; Casas, I.; Martínez, M.; Miralles, N.; Florido, A. *J. Hazard. Mater.* **2010,** *174*, 144.
10. Malkoc, E.; Nuhoglu, Y. *J. Hazard. Mater.* **2006,** *135*, 328.
11. Panda, G. C.; Das, S. K.; Guha, A. K. *J. Hazard. Mater.* **2009,** *164*, 374.
12. Asadullaha, M.; Asaduzzamana, M.; Kabira, M. S. *J. Hazard. Mater.* **2010,** *174*, 437.
13. Kumar, P. S.; Ramalingam, S.; Senthamarai, C.; Niranjanaa, M.; Vijayalakshmi, P.; Sivanesan, S. *Desalination* **2010,** *261*, 52.
14. Vimonses, V.; Lei, S.; Jin, B.; Chow, C. W. K.; Saint, C. *Appl. Clay Sci.* **2009,** *43*, 465.
15. Arslan, M.; Yigitoglu, M. *J. Appl. Polym. Sci.* **2008,** *107*, 2846.
16. Roy, A.; Chakraborty, S.; Kundu, S. P.; Basak, R. K.; Majumder, S. B.; Adhikari, B. *Bioresour. Technol.* **2012,** *107*, 222.
17. Vieira, A. P.; Santana, S. A. A.; Bezerra, C. W. B.; Silva, H. A. S.; Chaves, J. A. P.; Melo, J. C. P.; Filho, E. C. S.; Airoldi, C. *J. Hazard. Mater.* **2009,** *166*, 1272.
18. Al-Degs, Y. S.; Khraisheh, M. A. M.; Allen, S. J.; Ahmad, M. N. *J. Hazard. Mater.* **2009,** *165*, 944.
19. Deniz, F.; Karaman, S. *Chem. Eng. J.* **2011,** *170*, 67.
20. Chen, H.; Zhao, J. *Adsorption* **2009,** *15*, 381.
21. Rao, B. V. V.; Rao, S. R. M. *Chem. Eng. J.* **2006,** *116*, 77.
22. Oladoja, N. A.; Akinlabi, A. K. *Ind. Eng. Chem. Res.* **2009,** *48*, 6188.
23. Bhattacharyya, K. G.; Sharma, A. *J. Environ. Manag.* **2004,** *71*, 217.
24. Mall, I. D.; Srivastava, V. C.; Agarwal, N. K.; Mishra, I. M. *Chemosphere* **2005,** *61*, 492.
25. Hu, Z.; Chen, H.; Ji, F.; Yuan, S. *J. Hazard. Mater.* **2010,** *173*, 292.
26. Arslan, M.; Yigitoglu, M. *J. Appl. Polym. Sci.* **2008,** *110*, 30.
27. Dulman, V.; Simion, C.; Barsanescu, A.; Bunia, I.; Neagu, V. *J. Appl. Polym. Sci.* **2009,** *113*, 615.
28. Dou, X.; Zhang, Y.; Wang, H.; Wang, T.; Wang, Y. *Water Res.* **2011,** *45*, 3571.
29. Chatterjee, S.; Chatterjee, S.; Chatterjee, B. P.; Guha, A. K. *Colloids Surf. A* **2007,** *299*, 146.
30. Arulkumar, M.; Sathishkumar, P.; Palvannan, T. *J. Hazard. Mater.* **2011,** *186*, 827.
31. Saad, S. A.; Isa, K. M.; Bahari, R. *Desalination* **2010,** *264*, 123.
32. Martin, M. D. J.; Maria, P. E. G.; Virginia, H. M. *Bioresour. Technol.* **2009,** *100*, 6199.
33. Vimonses, V.; Lei, S.; Jin, B.; Chow, C. W. K.; Saint, C. *Chem. Eng. J.* **2009,** *148*, 354.